EVALUATION OF SILVER NANOPARTICLE-FORTIFIED BIOCHAR AS A REACTIVE FILTER MEDIA FOR IRRIGATION WATER DISINFECTION

by

Steven J. Lobo II

A thesis submitted to the Faculty of the University of Delaware in partial fulfillment of the requirements for the degree of Master of Civil Engineering

Spring 2019

EVALUATION OF SILVER NANOPARTICLE-FORTIFIED BIOCHAR AS A REACTIVE FILTER MEDIA FOR IRRIGATION WATER DISINFECTION

by

Steven J. Lobo II

Approved: _____
Pei C. Chiu, Ph.D.
Professor in charge of thesis on behalf of the Advisory Committee

Approved: _____
Sue McNeil, Ph.D.
Chair of the Department of Civil and Environmental Engineering

Approved: _____
Levi T. Thompson, Ph.D.
Dean of the College of Engineering

Approved: _____
Douglas J. Doren, Ph.D.
Interim Vice Provost for Graduate and Professional Education

ACKNOWLEDGMENTS

I would like to thank my advisor Dr. Pei Chiu, for his guidance and expertise which assisted me greatly throughout this research project. I would like to recognize Danhui Xin for all the help she has given me inside and outside of the lab. I want to thank Leslie Ope, Camila Babativa, and Elijah Akanbi for their help in the lab assisting me with my experiments. I would also like to recognize my colleagues in the Chiu and Chin research groups for their insight and assistance. I would also like to acknowledge the Department of Civil and Environmental Engineering.

I want to extend a thank you to my family and friends for their continued support throughout my academic endeavors. I also want to extend a thank you to my girlfriend, Emily Baranowski, for supporting me every day throughout my thesis research.

Lastly, I would like to thank my funding agencies, the United States Department of Agriculture and National Institute of Food and Agriculture, as well as the CONSERVE research group for the opportunity to pursue this research and my degree.

TABLE OF CONTENTS

LIST OF TABLES

LIST OF FIGURES

ABSTRACT

Despite increased governmental efforts, foodborne illnesses persist as a major risk to public health in the United States. With increasing demand for fresh vegetables and produce, contaminated crops are one of the most common sources of foodborne illnesses. One common crop contamination pathway is contaminated irrigation water. In an effort to combat the issue of foodborne illnesses, the U.S. Food and Drug Administration introduced new regulations targeting the food production industry, including a stricter law regarding the allowable amount of bacteria in irrigation water. Given these regulations and increasing water scarcity due to climate change, it is imperative that farmers have a simple and reliable way to treat their irrigation water.

This work focuses on the removal of *Escherichia coli* from irrigation water using a novel water treatment media, silver-amended soil reef biochar (Ag/SRB). Biochar is produced from pyrolyzed organic waste and has been used in water treatment applications for chemical removal and transformation. Through addition of silver, Ag/SRB can significantly reduce microbial concentrations in water, unlike plain biochar. Experiments were conducted to assess Ag/SRB's ability to reduce *E. coli* cell concentrations under batch system conditions and were compared with batch inactivation experiments using $AgNO_3$-derived silver ion (Ag+). It was determined that 0.1 g/L and 1 g/L Ag/SRB could remove 1.5 log and 3 log of *E. coli*, respectively, following 30 minutes of contact time. Ag+ measurements were taken during Ag/SRB

batch experiments and the predicted inactivation rates given the Ag+ concentrations were comparable to the results of the Ag+ inactivation experiments. Ag/SRB was also used in a flow-through column system and compared with unamended biochar. With a retention time of two minutes, Ag/SRB was able to remove 0.75 log of *E. coli* from an *E. coli* spiked wastewater effluent. These results demonstrate that Ag/SRB has the potential to be an effective irrigation water treatment media

Future research should focus on studying the longevity of Ag/SRB and how removal performance changes over time. Different flow rates and water matrices should also be explored to assess potential effects on Ag/SRB's performance.

Chapter 1

INTRODUCTION

Foodborne illness outbreaks are a major health concern throughout the United States and the world. The Centers for Disease Control and Prevention (CDC) estimate that 76 million foodborne illnesses occur in the United States every year (Nyachuba, 2010). Food contamination can occur at every step in the food production process, from the farmer's field to the consumer's dining table. Despite numerous efforts to reduce the amount of foodborne illnesses in the United States from multiple national agencies, the problem persists. In fact, the number of annual foodborne disease outbreaks and foodborne illnesses reported to the CDC have remained generally constant, in recent decades, despite increasing efforts to lower these numbers (Nyachuba, 2010). Several factors are likely leading to this including: increased consumption of fresh fruit and vegetables, large-scale production and wide distribution of food, and globalization of the food supply (Jung, Jang, Matthews, 2014); (Nyachuba, 2010). To protect consumers, government agencies continue to explore new tactics with the goal of reducing foodborne illness.

While food safety education programs targeting consumers have taken place, most governmental efforts have been focused on food producers and processors. One such of these recent efforts was the Food and Drug Administration's (FDA) Food Safety Modernization Act (FSMA) which was signed into law in 2011 (Center for Food Safety and Applied Nutrition, 2018). Among other regulations within FSMA, is an increased restriction regarding the allowable amount of generic *E. coli*, an indicator

organism for overall microbial contamination, in irrigation-use water. Specifically, the geometric mean of a minimum of 20 samples, for untreated surface water, and four samples, for untreated groundwater, of irrigation-use water must contain less than 126 colony-forming units (CFU) of generic *E. coli* per 100 mL of water (Center for Food Safety and Applied Nutrition, 2018). This, combined with other regulations, increases economic burdens on farmers, particularly smaller-scale farmers with tighter budgets as they may need to invest in equipment and other resources to meet these new standards.

Agricultural irrigation uses a lot of fresh water. Roughly 39% of the fresh water used in the United States is consumed irrigating crops (Perlman and USGS, 2016). With increasing urbanization and rising populations, demand for crops continues to rise as well. This makes it imperative that farmers have a steady water supply. Increased drought and climate variability due to climate change are serious threats to the water security of many farmers in the United States (McDonald et. al, 2011). Water scarcity combined with increased regulation, which further limits the waters that farmers can use to irrigate their crops, puts farmers in a difficult position.

Many farms have access to surface waters in the form of lakes, ponds, or rivers that may not meet current standards to be employable as irrigation-use water. Some farms also process their fruit and/or vegetables on-site. Much of the water used in this process becomes microbially contaminated and thus unsuitable for irrigation use and is, subsequently, piped to the local wastewater treatment plant. Many of these waters could be treated on-site and used in addition to a farm's primary irrigation water source. This would reduce water waste and increase a farm's available water supply. However, conventional water treatment systems can be quite costly, producing an

economic barrier for small and mid-scale farmers. For this reason, it is important to work towards developing a cost-effective and easy-to-use water treatment system that smaller farms could use to improve their water security.

A possible solution to this problem would be developing a disinfecting filter media for on-site water treatment. To maintain low costs, this media should be prepared using low-cost renewable materials. One of these low-cost materials could be biochar, which is produced from the pyrolysis of organic waste material. While raw biochar lacks the ability to disinfect water, the recent invention of a silver nanoparticle-modified biochar shows promise to serve as a low-cost effective water disinfection media that would be suitable for on-site water treatment. The purpose of this study is to investigate this novel potential water treatment media, silver-amended soil reef biochar (Ag/SRB), that may be able to address these issues, providing a simple way for farmers to treat microbially contaminated water that could then be used to irrigate their crops. This treatment media utilizes biochar as the base support. Biochar is a carbon-rich product produced by heating biomass in the absence of or with limited air to above 250°C (Lehmann and Joseph, 2015). Biochar is then chemically treated and amended with silver in a process described in Chapter 3.2. The resulting product, silver-amended biochar, serves as a silver repository in the form of zero-valent silver nanoparticles bound to the biochar surface and pores and sorbed silver ion. The goals of this study are as follows: (1) Evaluate silver ion toxicity to *E. coli* 353 TVS under batch system conditions (2) Evaluate Ag/SRB's ability to inactivate *E. coli* 353 TVS under batch system conditions and compare with silver ion toxicity (3) Investigate Ag/SRB's ability to inactivate *E. coli* 353 TVS in a natural surface water matrix under column system conditions.

Chapter 2

LITERATURE REVIEW

2.1 Silver Nanoparticle and Silver Ion (Ag+) Toxicity to Microorganisms

Silver has been long known to be an excellent antimicrobial agent. It is commonly used, in the form of silver nitrate ($AgNO_3$), in medical applications for the treating of diseases/infections caused by bacteria, fungi, and viruses (Zhang et. al, 2016). Silver has also been occasionally applied in water distribution systems for the inactivation of pathogens (Hwang et. al, 2007). Silver ion interacts with microorganisms in a variety of ways, with McDonnell and Russell (1999) asserting that the primary biocidal mechanism was related to the interaction of silver with thiol groups in enzymes and proteins.

Given these strong antimicrobial properties, there has been increasing interest in silver due to the development of high-quality silver nanoparticles over the past few decades. Silver nanoparticles (AgNPs) exist in a zero-valent (Ag^0) form with a size of less than 100 nm for each individual particle (Zhang et. al, 2016). Due to their strong antimicrobial properties, AgNPs are also being used in medical applications as well as in some consumer products. AgNPs can serve as long-lasting antimicrobial agents under harsh environmental conditions and can be synthesized in a variety of ways depending on the application (Ivask et. al, 2014). AgNPs effectively serve as a repository for silver ions which are slowly released through Ag^0 oxidation (Liu and Hurt, 2010).

It has been largely agreed upon in the scientific community that the toxicity of AgNPs is overwhelming due to the release of toxic silver ions (Zhang et. al, 2015). Most closely related to this study, Xiu et. al (2012) exposed *E. coli* cells to AgNPs under aerobic and anaerobic conditions. Their results showed significant *E. coli* inactivation under aerobic conditions, with minimal inactivation observed under anaerobic conditions. This led them to conclude that the toxicity of AgNPs is due to Ag+ release through oxidation of Ag^0 with minimal particle-specific effects. Another study that focused on AgNP and Ag+ toxicity towards a unicellular alga, *E. gracilis*, in liquid growth media showed that the EC_{50}'s (concentration of a toxicant that gives half-maximal response) for AgNPs and Ag+ were comparable (Zhang and Wang, 2018). In this same study, cysteine, a strong silver ligand, was also added in excess in a separate experiment to bind with Ag+ released from AgNPs and minimal growth inhibition was observed. These results along with the results of many other studies indicate that AgNP toxicity is due to release of silver ion.

2.2 Applications of Biochar in Water Treatment

Biochar is a carbon-rich product produced by heating biomass in the absence of or with limited air to above 250°C. Biochar is commonly used as a soil amendment to increase soil fertility. Biochar's generally high specific surface area increases the volume of water and air that can be held in a soil, making it more favorable for plant and microbial life (Lehmann and Joseph, 2015). While biochar is commonly used as a soil amendment, in recent years there has been increasing interest in using biochar to remove chemical contaminants from contaminated water.

Using pinewood and rice husk-derived biochars produced through hydrothermal liquefaction, Liu and Zhang (2009) demonstrated that biochar can be

used to remove lead (Pb) from aqueous solutions. The pinewood and rice husk biochars were able to remove 4.25 mg Pb/g and 2.40 mg Pb/g, respectively. Through modification of hickory wood-derived biochar with sodium hydroxide, Ding et. al (2016) demonstrated removal of lead, copper, cadmium, zinc, and nickel from aqueous solutions, however, this removal was only significant with lead and copper. Lastly, Yao et. al (2011) removed phosphate substantially from aqueous solutions over a range of pH and ionic conditions using a sugar beet tailing-derived biochar. As can be seen, biochar can come from many different feedstocks and can be prepared and amended in a variety of ways with researchers developing new methods all the time.

Biochar has not been substantially explored as a potential media for treatment of microbial contamination in water. Using a biochar-augmented sand biofilter, Mohanty and Boehm (2014) demonstrated 95% removal of *E. coli* from stormwater in a flow-through column system. However, this removal dropped to 62% when fine (<125 μm) biochar was removed, indicating that removal efficiency decreases with increasing particle size. A study was completed to assess the impact of biochar addition on *E. coli* populations in soils, but this has little relevance to how biochar would perform in a water treatment scenario (Gurtler et. al, 2014).

2.3 Applications of Zero-Valent Iron in Water Treatment

Zero-valent iron (ZVI) is a cheap, non-toxic, and effective reductant. It can be produced from steel shavings from a steel mill in the form of bulk aggregate or can be produced as nano-scale particles depending on the application (Fu et. al, 2014). ZVI can transform chemical contaminants through electron transfer and by sorbing contaminants. ZVI can transfer electrons to oxidized contaminants, for example, the

toxic and highly mobile Chromium (VI) (Cr(VI)), reducing it to Cr(III) which is less toxic and less mobile thus posing a reduced risk to human health (Fu et. al, 2014).

Given ZVI's ability to transform toxic contaminants, there has been significant interest in using ZVI to treat contaminated groundwater and wastewater over the past several decades. Arsenic is a toxic chemical that is commonly found in groundwater. Sun et. al (2006) demonstrated that ZVI can remove arsenate (Ar(V)) from water with 98% removal efficiency in a column system with a hydraulic retention time of 2 hours. ZVI has also been shown to dechlorinate chlorinated organic compounds, which are resistant to degradation and persist in the environment. One study showed that, in a batch system, ZVI reduced the concentration of pentachlorophenol by roughly 90% following 25 days of contact (Kim and Carraway, 2000). For these reasons, as well as being able to remove nitroaromatic compounds, nitrate, and dyes, ZVI has seen implementation in permeable reactive barriers for groundwater treatment.

ZVI has, similarly to biochar, not been explored significantly as a microbial contamination treatment media. This is likely due to ZVI's lack of inherently toxic properties. However, ZVI nanoparticles have been shown to reduce *E. coli* concentrations by 0.82 log/mg nano-Fe^0/L h under anaerobic conditions (Lee et. al, 2008). While ZVI, has not been demonstrated to be effective at removing bacteria, it has been shown to be effective at removing viruses and bacteriophages. ZVI was shown to remove 4 log of the bacteriophages φX174 and MS-2 from artificial groundwater in an initial pulse test and over 5 log following the passage of 320 pore volumes (You et. al, 2005). A packed ZVI column was also shown to remove 5 log of Aichi virus and 2.6 log of Adenovirus 41 from water treatment plant water (Shi et. al, 2012).

Chapter 3

EXPERIMENTAL METHODS

3.1 Chemicals and Materials

Silver nitrate (99.9+%) and sodium dithionite (85+%) were purchased from Alfa Aesar (Haverhill, MA). Sodium bicarbonate (99.7+%), sodium nitrate (99+%), nitric acid (trace metal grade), and dimethyl sulfoxide (99.7+%) were obtained from Fisher Scientific (Pittsburgh, PA). Tryptic Soy Agar and Tryptic Soy Broth growth media were obtained from Remel (San Diego, CA). Rifampicin (97+%) was purchased from Sigma Aldrich (St. Louis, MO). Phosphate Buffered Saline was acquired from Gibco (Dublin, Ireland). Sodium citrate (99+%) was purchased from Acros Organics (Somerville, NJ). All chemicals were used as received.

The biochar used in this work was purchased from Soil Reef LLC located in Berwyn, PA. This biochar is branded as Soil Reef Biochar (SRB) and is produced from pyrolyzed wood residues (Soil Reef LLC). SRB was chosen as it is an inexpensive commercially available biochar. All SRB was sieved to the 250 μm-500 μm particle size range. Physical characteristics of Soil Reef Biochar are shown in Table 3.1 (Nakhli et. al, 2019).

Table 3.1 Soil Reef Biochar Physical Characteristics

Parameter	Averaged Value	Standard Error
Skeletal Density (g/cm^3)	1.05	0.12
Envelop Density (g/cm^3)	0.52	0.03
N_2 BET Surface Area (m^2/g)	355	6
Ash Content (% mass)	10.56	0.18
Carbon (% mass)	76.8	0.7
Hydrogen (% mass)	0.83	0.014
Nitrogen (% mass)	1.87	0.02
Sulfur (% mass)	0.25	0.00
Oxygen (% mass)	9.7	0.7

Cast iron aggregate (zero-valent iron (ZVI)) was purchased from Peerless Metal Powders and Abrasives in Detroit, MI. ZVI was sieved to the same particle size range as SRB, 250 μm-500 μm.

3.2 Silver-Amended Soil Reef Biochar Synthesis and Specifics

Silver-amended soil reef biochar (Ag/SRB) was developed and produced by Danhui Xin, a PhD. student in Dr. Pei Chiu's lab group at the University of Delaware. A detailed explanation of the Ag/SRB production process will be available in a soon to be released scientific paper focused on the subject. This synthesis process is currently protected under a provisional patent: Chiu, P. C., Xin, D. and Lobo, S. "A Method to Prepare Silver-Amended Carbon Sorbents for Drinking Water and Irrigation Water Treatment." Provisional applications filed 05/03/18 (serial number

62/666,336) and 07/13/18 (serial number 62/697,428). A simplified description of the synthesis process will follow.

All Ag/SRB preparation was performed in an anaerobic glove box (2.0±0.5% H_2 in 98% N_2, P_{O_2}<25 ppm, Coy, MI). SRB was ground to <100 μm particle size fraction. Silver addition was achieved through a two-step process: (1) SRB was reduced with dithionite, and (2) silver was added to reduced SRB in a pH-controlled solution. Specifically, pre-oxidized SRB (with dissolved oxygen, for 72 h) was reduced with dithionite in a citrate buffer at pH 6.4 for three days. Freshly prepared dithionite solution was added in excess and replenished as needed to ensure complete reduction of SRB. Reduced SRB was collected on a glass fiber filter, rinsed thoroughly with deoxygenated deionized water to remove any residual dithionite, and vacuum-dried before exposure to silver.

A known mass of SRB was suspended in a 200 mL $NaNO_3$ solution in a 1–L amber bottle on an orbital shaker at 100 rpm. After equilibration for 30 min with $NaNO_3$ solution, an aliquot of 100 mM $AgNO_3$ was added to initiate silver addition to SRB. Aqueous Ag+ concentrations were monitored continuously using an Ag+ ion selective electrode (ISE) and an ISE meter (Cole–Parmer, IL). As uptake of Ag+ proceeded and its concentration dropped to <1 mM, another aliquot of $AgNO_3$ would be added to maintain the Ag+ concentration. Solution pH was maintained at a predetermined value (±0.4 pH unit) throughout each experiment using a pH controller (Bluelab, NZ). The addition of a base (NaOH) was needed in order to compensate for pH decrease due to the release of protons. The silver loading of SRB was calculated

based on mass balance using Eq.1. Addition of silver was taken to be at equilibrium when the change between two consecutive measurements was <3%. The product, Ag/SRB, was retrieved on a glass microfiber filter, vacuum-dried, and stored in a desiccator in the glove box.

$$Ag\ loading\ (mmol) = C_{AgNO_3} \times jV_{AgNO_3} - C_i \times (V_{NaNO_3} + jV_{AgNO_3} + V_{NaOH}) \qquad (1)$$

where C_{AgNO3} and C_i are the Ag+ concentration of the stock solution (100 mM) and the reactor at the ith measurement, respectively; j is the total addition of $AgNO_3$ aliquots; V_{NaNO3}, V_{AgNO3}, and V_{NaOH} are the initial volume of the reactor (200 mL), and the volume of each $AgNO_3$ aliquot and base, respectively.

Ag/SRB with silver loading of 2.289 mmol/g and 1.0 mmol/g were used in this study. Silver loading onto air-oxidized SRB was also measured to determine how much Ag+ could sorb to untreated SRB. It was determined that this Ag+ sorption was 0.267 mmol/g.

3.3 Microorganism of Interest and Growth Conditions

3.3.1 Microorganism of Interest

Escherichia coli 353 TVS was chosen as the test organism for this study. *E. coli* 353 TVS was isolated from surface irrigation water in the Central Coast region near Salinas, California (Tomás-Callejas et. al, 2011). This non-pathogenic persistent environmental *E. coli* strain was chosen as a surrogate for pathogenic *E. coli* by the CONSERVE research group due to its relevance to one of the research group's goals

of treating microbially contaminated surface waters to comply with standards for irrigation use (CONSERVE, 2016). A pure *E. coli* 353 TVS culture plate was received from the Dr. Manan Sharma research group at the USDA Agricultural Research Laboratory in Beltsville, MD. This *E. coli* strain is naturally resistant to the antibiotic, rifampicin, at concentrations up to 80 μg/mL (Sharma et. al, 2016).

3.3.2 Growth Conditions and Media Preparation

3.3.2.1 Liquid Cultures

All *Escherichia coli* 353 TVS liquid cultures were grown in a Tryptic Soy Broth (TSB) and 80 μg/mL rifampicin solution. The growth solution is prepared by fully dissolving the TSB powder in deionized water (DI) as directed. Once thoroughly stirred, the TSB solution was autoclaved at 121°C under 15 psig for 15 minutes for sterilization. After autoclaving, the TSB solution is sealed and allowed to cool. Once cool, 24.975 mL of the TSB solution is pipetted into a 50 mL sterile centrifuge tube. Following this, 25 μL of an 80 mg/mL rifampicin stock solution is added and the tube is then vortexed. A single ice crystal is then removed from a frozen *E. coli* culture using a sterile inoculating loop and dispersed in the growth solution. The growth solution is then vortexed again and placed in an incubator at 37°C for 24 hours allowing the cell concentration to reach ~10^9 CFU/mL (Sharma et. al, 2016). Following incubation, the liquid culture is stored in the refrigerator at 4°C and can be used in experiments for up to 6 weeks.

3.3.2.2 Frozen Cultures

Frozen *E. coli* cultures are prepared in a similar fashion as the liquid cultures; however; they require the addition of glycerol to their growth solution. Glycerol is added to reduce the risk of *E. coli* cells being damaged by ice crystals in the freezing/thawing process. Frozen cultures are made in 2.5 mL cryogenic vials and consist of 1.8 mL of the growth solution described in Chapter 3.3.2.1 with the addition of 0.2 mL of glycerol. This solution is vortexed. The solution is then inoculated using a sterile inoculating loop to remove a single colony from the pure *E. coli* 353 TVS culture plate described in Chapter 3.3.1 and dispersing the single colony in the growth solution. The frozen culture is then sealed and incubated at 37°C for 24 hours. After incubating, the frozen culture is stored in the freezer at -20°C and can be used to inoculate liquid cultures for up to one year.

3.3.2.3 Growth Plates

Growth plates were used in this study to quantify *E. coli* 353 TVS concentrations in terms of colony-forming units per mL (CFU/mL). Growth plates were prepared using sterile 100 mm x 15 mm polystyrene petri dishes. Tryptic Soy Agar (TSA) was used as the solid growth media for this work. TSA powder was added to DI water as directed and then placed on a hot plate with a magnetic stirrer. This mixture is then heated and stirred until the agar particles fully dissolve, turning the cloudy mixture into a clear solution. This indicates that the solution is now ready to be used to make agar plates. Following this, the solution is autoclaved at 121°C and 15

psig for 15 minutes to sterilize the liquid media. Once removed from the autoclave, the liquid media is sterile and ready to be poured into plastic petri dishes. Each dish receives 15-20 mL of the liquid media. Once poured, the plates are left to sit for 20-30 minutes. After this time, the plates will have solidified and can now be stored for later use in the refrigerator for roughly two weeks.

3.3.2.4 Phosphate Buffered Saline Solution

Phosphate Buffered Saline (PBS) was chosen as the dilution liquid for this study (Tomás-Callejas et. al, 2011). PBS has the ability to stabilize bacterial cells and contains little organic matter meaning that cell concentrations should remain constant following contact. PBS solution was prepared as directed by dissolving PBS powder in DI water. After stirring until full solvation, the PBS solution was then autoclaved at 121°C and 15 psig for 15 minutes. After being allowed to cool, the autoclaved PBS solution can now be used for a variety of applications in this study.

3.4 Liquid Culture Centrifugation and *E. coli* Quantification Method

3.4.1 *E. coli* Liquid Culture Centrifugation

Liquid cultures were centrifuged prior to use in experiments due to concerns that the high organics concentration associated with the TSB may influence how Ag+ and Ag/SRB interact with *E. coli* cells. Firstly, a 5 mL sample from a liquid *E. coli* culture was taken and placed in a centrifuge cuvette. This cuvette was then centrifuged at 5000 rpm for 10 minutes at 25°C (Tomás-Callejas et. al 2011). Upon removal from

the centrifuge, the supernatant is extracted, leaving a large cell pellet at the bottom of the cuvette. Generally, 4.9 mL of supernatant is removed and then replaced with an equivalent amount of PBS to maintain the pre-centrifugation cell concentration. With the PBS added, the cuvette is then vortexed to resuspend *E. coli* cells. With most of the TSB removed, the liquid culture can now be used in inactivation experiments.

3.4.2 Quantification of *E. coli* Concentrations

E. coli concentrations were measured by diluting samples, spreading them on growth plates, and counting visible colonies on growth plates following incubation. *E. coli* samples require dilution due to the physical limitations of growth plates. Too few colonies on a growth plate may result in an inaccurate cell calculation, while too many colonies can crowd the growth plate, making counting of individual colonies very difficult. For this reason, a "countable plate", or a growth plate where the number of visible colonies on it can be easily distinguished and thus can serve as a reliable measurement of colony-forming units in the original system, was considered to be a growth plate with 10-300 visible colonies. As stated, dilutions had to be made in order to obtain a countable plate for *E. coli* concentrations that can vary from 200 CFU/mL (the detection limit for measuring *E. coli* concentrations in this study) to $3 * 10^9$ CFU/mL. This diluting occurred by first taking a raw 1.0 mL sample from the reactor of interest and not diluting the sample (10^0). Secondly, a 1.0 mL sample would be taken again and then added to a sterile 15 mL centrifuge tube containing 9.0 mL of sterilized PBS. This tube would then be sealed and vortexed, making this a dilution of

one order of magnitude (10^{-1}). Following this, 1.0 mL would be drawn from the 10^{-1} tube and dispersed into another centrifuge tube containing 9.0 mL of PBS. This would also be vortexed and now the original sample had been diluted by two orders of magnitude (10^{-2}). This dilution process would be repeated until one believed the sample had been sufficiently diluted to yield a countable plate.

Following desired sample dilution, 0.1 mL from a dilution tube would be drawn and deposited on the surface of a growth plate. This would then be spread to fully cover the surface of the growth plate using a sterile inoculating loop. All samples taken during experiments were plated in duplicate to ensure accuracy with the exception of samples taken just before the start of an experiment which were used to determine the initial *E. coli* concentration. These initial concentration samples were plated in triplicate for increased accuracy. Following spreading, plates were covered, labeled with their corresponding dilution factor, and then incubated at 37°C for 48 hours.

After incubation, colonies were counted on plates using a colony counter pen. As stated previously, 0.1 mL of a sample is spread on growth plates, however, cell concentrations are measured in CFU/**mL**. To address this, all colony counts were raised an extra order of magnitude in addition to their dilution factor when back-calculating. For example, if 50 colonies were counted on a 10^{-2} growth plate, the cell concentration would be $5 * 10^4$CFU/mL. An example showing *E. coli* 353 TVS growth on TSA plates at different dilution factors is shown in Figure 3.1. Each individual cloudy dot represents a colony-forming unit.

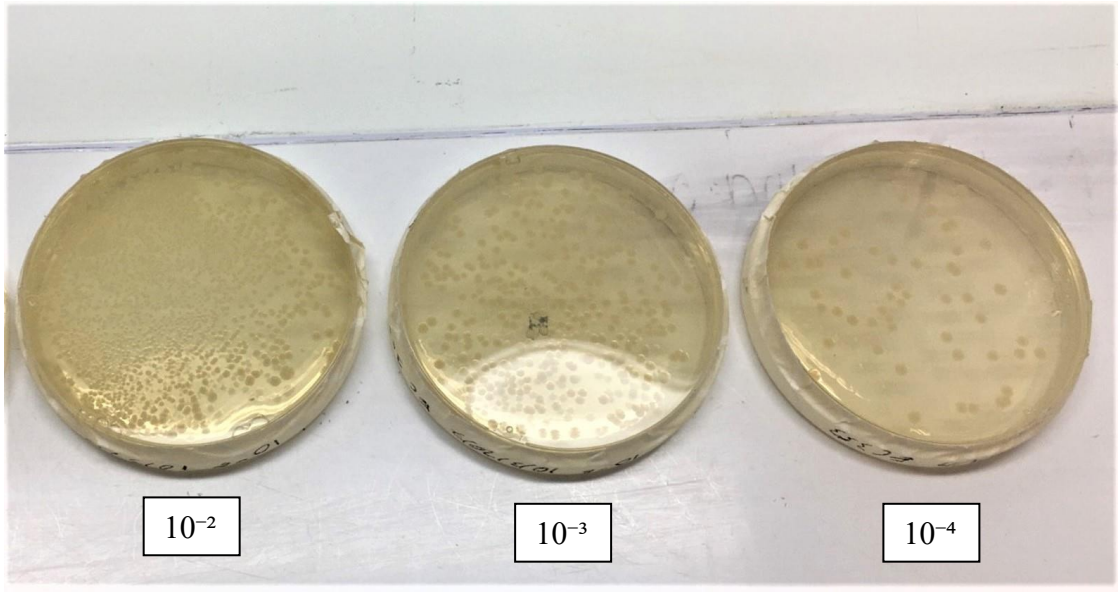

Figure 3.1 *E. coli* 353 TVS growth on TSA plates, Number of colonies decreases with increasing dilution (left to right)

3.5 Ionic Silver (Ag+) Measurement

In addition to *E. coli* 353 TVS cell concentrations, ionic silver concentrations were also measured during silver-amended soil reef biochar inactivation experiments. While the silver that is bound to the biochar in Ag/SRB exists in the form of zero-valent silver (Ag(0)) nanoparticles, it is believed by many that the biocidal activity of zero-valent silver nanoparticles is due to the release of Ag+ from these nanoparticles (Zhang et. al, 2015), (Zhang and Wang, 2018). Given this, it was deemed useful to measure the Ag+ concentration of Ag/SRB containing reactors for the purposes of comparing *E. coli* inactivation by Ag/SRB to inactivation by Ag+. During batch

Ag/SRB inactivation experiments, Ag+ samples were always taken 5 minutes after the start of the experiment and then samples were subsequently taken at the same times at which *E. coli* samples were taken. Ag+ concentrations were measured using Inductively Coupled Plasma Mass Spectrometry (ICP-MS). An Agilent 7500C ICP-MS located in Room 150 of DuPont Hall at the University of Delaware in Newark, DE was used for this analysis.

The Ag+ sampling process consisted of taking a 0.5 mL sample from a Ag/SRB containing reactor during an *E. coli* inactivation experiment and storing that sample in a 15 mL centrifuge tube until the experiment was completed, allowing for the experiment to finish. Following this, a 5 mL syringe with a luer-lock tip would have its plunger removed and sat aside. Then a 0.22 μm PVDF syringe filter is fixed on the luer lock tip. The 0.5 mL sample is then poured into the syringe and pushed through the syringe filter using the plunger into a new 15 mL centrifuge tube containing 2 mL of 2% nitric acid (HNO_3). All ICP-MS samples require filtration using a 0.22 μm filter and digestion using 2% HNO_3 to remove large particles and break up aggregates, respectively. With the 0.5 mL sample filtered through, an additional 2.5 mL of 2% HNO_3 is added to the original 15 mL centrifuge tube that held the 0.5 mL sample and the tube is then vortexed. This 2.5 mL is then poured into the same syringe as the 0.5 mL sample and filtered through the same syringe filter into the 2.5 mL Ag+/HNO_3 containing tube, making the final volume 5 mL. This tube rinse and filtration with the 2.5 mL 2% HNO_3 is done to reduce sample loss due to cohesion in the original sample tube and sample retention in the syringe filter. As can be seen,

once this process has finished the Ag+ sample has been diluted by a factor of 10. Once all Ag+ samples are processed in this way, a Ag+ calibration curve must be prepared. Calibration standards were prepared using $AgNO_3$ as the Ag+ source with concentrations of 0, 5, 10, 50, and 100 parts per billion (ppb). These standards were prepared similarly to Ag+ samples with 2 % HNO_3 serving as the solvent and all standards being filtered using 0.22 μm PVDF filters. Samples can now be analyzed using ICP-MS with resulting concentrations, in ppb, being converted to molar units for comparison with Ag+ inactivation experiment data.

Ag+ samples from Ag/SRB inactivation experiments were originally measured using a slightly different method than the one described above that, upon later consideration, was deemed to have resulted in underestimations of the actual Ag+ concentration. This underestimating method involved filtering a 0.5 mL Ag+ sample into 4.5 mL of 2% HNO_3. As can be seen, it is likely that a non-negligible amount of the 0.5 mL sample was retained on the 0.22 μm filter, thus leading to less than 0.5 mL of the Ag+ being digested by the 2% HNO_3. To remedy this inaccuracy, the two methods were compared and a correction factor was calculated. All Ag+ measurements from Ag/SRB inactivation experiments reported in this study were multiplied by this correction factor, 1.198±0.204.

3.6 Batch *E. coli* 353 TVS Inactivation Experiments

All *E. coli* inactivation experiments were conducted in a non-bypass fume hood with the sash lowered to prevent excessive air flow. The fume hood interior was sanitized using 70% ethanol solution before setup for each experiment.

All batch system *E. coli* inactivation experiments were conducted in 125 mL capped amber bottles. Amber bottles were cleaned thoroughly and autoclaved at 121°C and 15 psig for 15 minutes prior to use in experiments. Batch experiments utilized a 10 mM sodium bicarbonate ($NaHCO_3$) ionic solution as the background aqueous environment to simulate a natural water. This solution was prepared by dissolving $NaHCO_3$ powder in DI water and autoclaving before use. Once autoclaved, the 10 mM $NaHCO_3$ solution was pH adjusted to 7.05±0.05 using concentrated HNO_3.

3.6.1 Inactivation Experiments using Ag+

A 1 mM $AgNO_3$ stock solution was used as the Ag+ source for these inactivation experiments. Ten minutes prior to the start of an experiment, 0.1 mL of centrifuged *E. coli* 353 TVS liquid culture was added to 98.4 mL-99.8 mL of 10 mM $NaHCO_3$ in an amber bottle and swirled. This was done to allow the *E. coli* cells to stabilize in their new aqueous environment, ensuring that any inactivation that occurs during the experiment would be due to addition of Ag+. After 10 minutes have passed, 0.1-1.5 mL of 1 mM $AgNO_3$ solution is then added, depending on the desired aqueous silver concentration for the reactor. The total solution volume of each reactor is 100 mL. Silver addition to the reactors marks the start of the experiment and,

subsequently; reactors are capped and swirled on a rotator at 100 rpm for the duration of the experiment.

Each inactivation experiment featured a “blank” reactor which consisted of 99.9 mL of 10 mM $NaHCO_3$ solution, pH adjusted to 7.05±0.05, and 0.1 mL of the centrifuged *E. coli* liquid culture. It was expected that over the course of an inactivation experiment there would be little to no change in cell concentration in this blank reactor. The purpose of this reactor was to confirm that any decrease observed in the Ag+-containing reactors was due to the addition of Ag+. For all Ag+ inactivation experiments, a sample was taken from this blank reactor once the experiment was started and the resulting cell concentration from this sample was assumed to be the initial cell concentration for all reactors. *E. coli* samples were taken from each reactor at three times throughout the experiment to measure the extent of inactivation.

3.6.2 Inactivation Experiments using Silver-Amended Biochar (Ag/SRB)

Batch inactivation experiments using Ag/SRB were conducted similarly to experiments using Ag+ as described in Chapter 3.6.1. These experiments also used 10 mM $NaHCO_3$, pH adjusted to 7.05±0.05, as the background aqueous solution. Ag/SRB substituted Ag+ as the biocidal agent for these experiments. A visual comparison between unamended SRB and Ag/SRB is shown in Figure 3.2. Note the larger amount of ash (very fine particles) in the unamended biochar on the left when compared to the Ag/SRB on the right. Even though the SRB was sieved, some small ash particles are likely still bound to larger SRB particles. Most of this bound ash was removed from

Ag/SRB due to the silver treatment process and subsequent washing. Also note that the SRB is slightly darker, also likely due to the higher ash content.

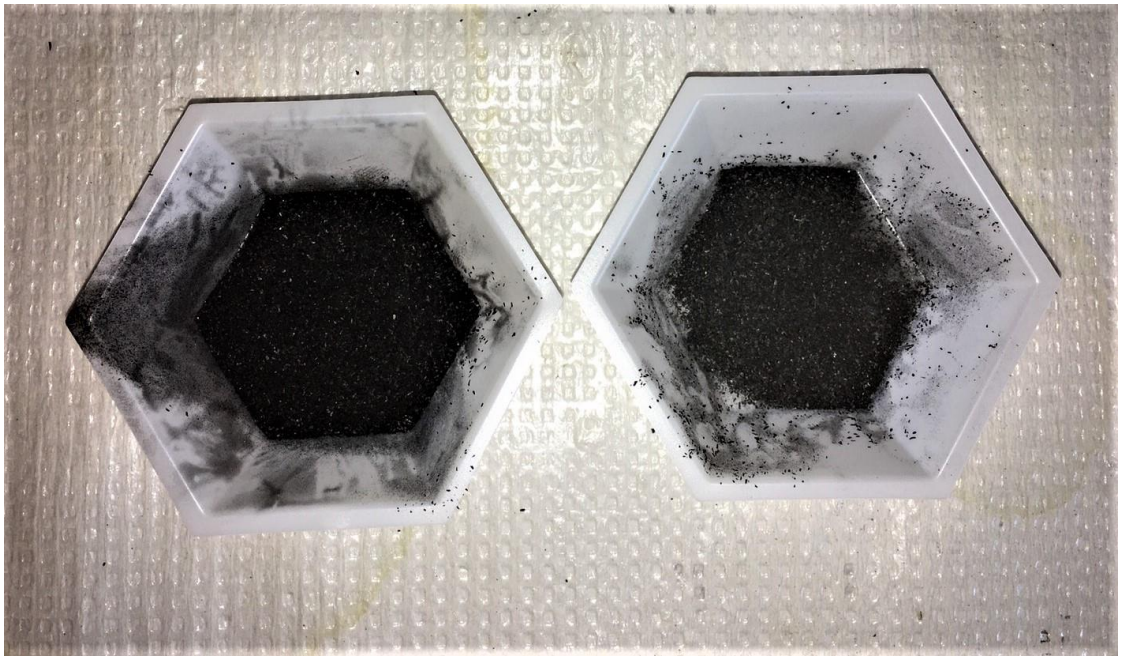

Figure 3.2 Unamended SRB (left) and Ag/SRB (right)

The Ag/SRB used in these experiments was loaded with 2.289 mmol Ag/gram. The work of Danhui Xin, a PhD. student in Dr. Pei Chiu's research group who produces and characterizes Ag/SRB for these experiments, indicates that Ag/SRB leaches silver ion when immersed in water. Her work shows that the Ag+ concentration leached from Ag/SRB in solution reaches a stable concentration after 60 minutes of immersion. For this reason, each mass of Ag/SRB being tested would be

immersed in 50 mL of pH 7, 10 mM $NaHCO_3$ solution in an amber bottle and placed on a rotator at 100 rpm for one hour before the start of an experiment. After 50 minutes of leaching had passed, 0.1 mL of a centrifuged *E. coli* liquid culture would be added to 49.9 mL of pH 7, 10 mM $NaHCO_3$ solution in a separate amber bottle. This bottle is swirled and capped. This is done to allow the *E. coli* cells to stabilize in this new aqueous environment before being exposed to the biocidal agent, Ag/SRB, and its leached Ag+. Once the one hour of Ag/SRB leaching has finished, the 50 mL *E.coli* solution has been allowed to stabilize and is poured into the 50 mL Ag/SRB containing reactor marking the start of the inactivation experiment.

E. coli samples were taken throughout each experiment from each reactor at various times. In addition, Ag+ samples were taken to measure Ag+ concentrations in each reactor at these same times. These Ag+ samples were processed as described in Chapter 3.5. Reactors containing SRB were also tested to serve as a control for direct comparison with the results of Ag/SRB containing reactors. ZVI was also used to investigate its ability to inactivate *E. coli* in a batch system. When any sample was taken from a reactor, extra care was taken to not remove any Ag/SRB, SRB, or ZVI particles from the reactor.

3.7 Flow-Through Column Experiments

3.7.1 Water Matrix

All column experiments were conducted using a wastewater treatment plant effluent collected from the Manchester Wastewater Treatment Plant in Manchester,

MD. This wastewater effluent was collected on February 27, 2019 by two researchers, Linyan Zhu and Suraj Panthi, from the College of Public Health at the University of Maryland in College Park, MD. This wastewater effluent was not chlorinated as the Manchester Wastewater Treatment Plant does not chlorinate their wastewater during the winter months. Wastewater water quality parameters are shown in Table 3.2 and were measured three times over the course of a year by researchers at the University of Maryland in the CONSERVE research group.

Table 3.2 Manchester Wastewater Treatment Plant Effluent Water Quality Parameters

Parameter	Averaged Value	Standard Deviation
Temperature (°C)	14.26	6.71
pH	7.28	0.12
Turbidity (FNU)	4.11	3.28
Nitrogen (mg/L)	11.25	9.03

The wastewater effluent was not autoclaved as the high temperature and increased pressure would alter the water chemistry. Thus, the wastewater effluent was filtered through 1 μm glass microfiber filters to remove bacteria and other microorganisms. The filtered wastewater effluent was then stored in a refrigerator at 4°C until needed for experiments. The filtered wastewater was then re-filtered just prior to being used in experiments.

3.7.2 Column Materials

3.7.2.1 Quartz Sand

Quartz sand was purchased from AGSCO Corporation in Pine Brook, NJ. The sand was pre-sieved by AGSCO to the particle size range of 177 μm-595 μm. The quartz sand was reported to contain 99.5% SiO_2 with a small 0.05% of iron hydroxides (AGSCO Corporation, 2016). To ensure that these iron hydroxides did not impact the removal efficiency of the sand, which is meant to be inert, showing minimal to no *E. coli* removal, the sand was chemically treated.

Iron hydroxides were removed following a modified version of a method described elsewhere (Mehra and Jackson, 1958). First, 500 g of quartz sand in a large Erlenmeyer flask is brought into an anaerobic glove box. The sand is then suspended in a 0.3 M sodium citrate and 0.1 M sodium dithionite solution. The dithionite fully reduces and solubilizes the iron hydroxides and, subsequently, the iron is then bound to the citrate. This is left overnight to ensure a complete process. The sand is then removed from the glove box in solution and placed in an incubator at 80°C for one day to remove any iron hydroxides that may have formed due to oxidation by the oxygen in the lab air. Following this, the sand is removed from the incubator and the solution supernatant is discarded. The sand is then rinsed with 5 L of DI water using a vacuum-filtration system to fully remove the citrate-dithionite solution. The treated sand is dried using a vacuum oven overnight. Following this, the sand can be stored until needed.

3.7.2.2 Soil Reef Biochar

Soil Reef Biochar was obtained as described in Chapter 3.1. SRB was left exposed to lab air for 24 hours to “air-oxidize” it. This was done to allow the SRB to

equilibrate with the lab air conditions to ensure consistent performance throughout the column experiments. Physical characteristics of Soil Reef Biochar are reported in Table 3.1

3.7.2.3 Silver-Amended Soil Reef Biochar

Ag/SRB was prepared as described in Chapter 3.2. Ag/SRB with silver loading of 1.0 mmol/g was used for all column experiments. All columns containing Ag/SRB in this study contained roughly 2 grams of Ag/SRB.

3.7.2.4 Glass Wool

Glass wool was purchased from Acros Organics in Somerville, NJ. Glass wool was used on both ends of each column to stabilize and evenly distribute water flow on the influent end and to prevent media particles from leaving the column on the effluent end. Glass wool is an inert substance that should not influence Ag/SRB or SRB performance in this study.

3.7.3 Column Construction

Individually wrapped, sterile BD 10 mL Luer-Lok Tip syringes were used as the small columns for this study. All columns were dry-packed, with the syringe plunger being used to compress column layers. The bulk densities of all column materials, except for glass wool, were measured to ensure consistent retention times for all treatment media for easy comparison of results. These bulk densities are reported in Table 3.3. All columns featured a small layer of glass wool on the bottom, a layer of treated sand on top of that, the media of interest (SRB or Ag/SRB), another

layer of sand, and then a top layer of glass wool. Packed columns were sealed at the top using a rubber stopper.

Table 3.3 Column Component Bulk Densities

Component	Bulk Density (g/cm^3)	Standard Deviation
Sand	1.177	0.041
Ag/SRB	0.356	0.019
SRB	0.212	0.003

Pore volumes (PVs), the total free space that water can flow through in a column, were measured by weighing the dry packed column, pumping DI water through the column for 2 hours to ensure complete saturation, weighing the saturated column, and then calculating the total volume of water using the difference in masses and the density of water. An example of a packed column is shown in Figure 3.3.

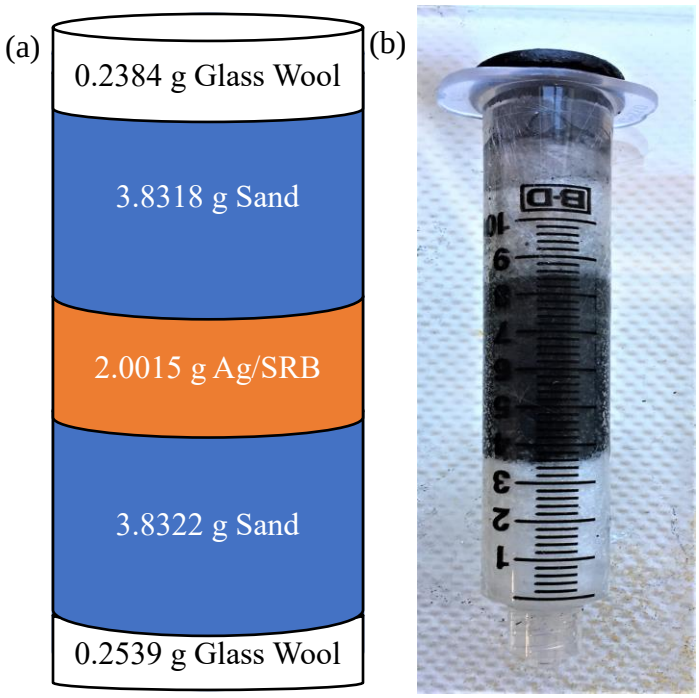

Figure 3.3 a) Schematic of a packed Ag/SRB containing column (not to scale) with mass values. b) Actual packed column with same mass values as (a)

3.7.4 Ag+ Leaching from Ag/SRB Column Experiments

All column experiments were performed using upflow pumping from the bottom to the top of the column. This was done to maintain steady flow rates by avoiding gravity driven flow. A Masterflex L/S 4-Channel Digital Pump System with Multichannel Head peristaltic pump was purchased from Cole Parmer in Vernon Hills, IL and used for the column experiments. All experiments were conducted at a flow rate of 2.5 mL/min. Masterflex L/S 16 BioPharm Plus Platinum-Cured Silicone Pump Tubing was used as the tubing for these experiments and was also purchased from

Cole Parmer. A sterile BD PrecisionGlide Needle was poked through the rubber cap at the top of each packed column to allow effluent collection.

Two identical columns were constructed as reported in Table 4.1. Both columns contained roughly two grams of Ag/SRB and similar amounts of sand and glass wool. Two column influents were prepared using 200 mL each of the filtered wastewater effluent. To observe potential differences in Ag+ leaching due to dissolved oxygen (DO) concentration, the two influents were either purged of or saturated with oxygen. To achieve a high DO concentration, one influent was continually pumped with air for two hours resulting in a DO concentration of 9.37 mg/L. Similarly, the other influent was purged with N_2 gas for two hours resulting in a DO concentration of 0.35 mg/L. Due to this pumping/purging, CO_2 was removed, making the pHs of both influents around 9.0. Roughly 100 mL (~20 PVs) of influent was pumped through each column.

Effluent samples (~5 mL each) were collected in sterile 15 mL centrifuge tubes using FRAC-100 fraction collectors with a sampling time of two minutes per sample. Effluent samples were then processed as described in Chapter 3.5 for Ag+ measurement using ICP-MS. All tubing connections were tight and no leaks were noticed during any column experiments.

3.7.5 *E. coli* Inactivation Column Experiments

These experiments were conducted under the same conditions as described in the first paragraph of Chapter 3.7.4 with some additional considerations. All tubing

was autoclaved at 121°C and 15 psig for 15 minutes before being used in any experiments involving *E. coli*. A single column influent was prepared for this experiment to ensure that both columns were receiving the exact same water. This influent consisted of 299.7 mL of filtered wastewater effluent and 0.3 mL of centrifuged *E. coli* stock that was diluted from a 10^9 CFU/mL stock to a 10^8 CFU/mL stock. With the 0.3 mL spike, this made the influent concentration of *E. coli* equal to roughly 10^5 CFU/mL. After the *E. coli* spike, the influent was well-stirred. A sample was then taken, diluted, and plated as described in Chapter 3.4.2. This later revealed the influent concentration was $1.72 * 10^5$ CFU/mL.

Two columns were constructed, one containing Ag/SRB and other containing SRB. Given the difference in densities of Ag/SRB and SRB, less SRB mass was used to ensure that both Ag/SRB and SRB occupied the same amount of volume in their respective columns and thus had the same contact time with *E. coli* cells. This is described in Chapter 4.3.2. The SRB-containing column was intended to serve as a control to isolate the effect of silver addition to Ag/SRB. Roughly 70 mL (~14 PVs) of influent was pumped through each column. Fifteen successive effluent samples were collected from each column using FRAC-100 fraction collectors. All effluent *E. coli* samples were diluted, plated, and incubated as described in Chapter 3.4.2.

3.8 Data and Statistical Analysis

All data for this work was logged and analyzed in Microsoft Excel 2016. Pseudo first-order rate constants were obtained by plotting data in scatter plots and

using Excel's built-in linear regression trendline function. R^2 values were also obtained in this manner. Curve fitting in Figures 4.3 and 4.5 was performed using the SOLVER add-in program for Microsoft Excel. Using SOLVER, optimization for these curves was achieved using non-linear regression analysis.

Chapter 4

RESULTS AND DISCUSSION

4.1 Batch System *E. coli* 353 TVS Inactivation Experiments using Ionic Silver

With one of the main goals of this work being to investigate the relationship between *E. coli* 353 TVS inactivation by Ag+ and Ag/SRB, it was decided to first explore *E. coli* inactivation by Ag+. It was believed that the results from Ag+ inactivation experiments would help inform how to design the following Ag/SRB inactivation experiments. An example experimental setup is shown in Figure 4.1

Figure 4.1 Ag+ Inactivation Experimental Setup

Experiments were conducted as described in Chapter 3.6.1. The results of these experiments are shown in Figure 4.2. Eight different Ag+ concentrations were tested ranging from 1-15 μM Ag+. A blank reactor was also tested and only minor *E. coli* concentration shifts were observed at sampling times. The *E. coli* concentrations in Figure 4.2 were normalized to make for easier comparison given that initial *E. coli* concentrations would fluctuate slightly from experiment to experiment. As expected, increasing Ag+ concentrations resulted in more rapid inactivation. Data points with error bars had at least two separate experiments where *E. coli* concentrations were able to be measured at the specified sampling time. This is why some data points may have an error bar while others may not for a single Ag+ concentration in Figure 4.2. Data was also only included in Figure 4.2 if it came from *E. coli* inactivation experiments where *E. coli* concentrations could be measured at three or more sampling times for a specific Ag+ concentration. All fitted trendlines were fit using linear regression and featured decreasing slopes with increasing Ag+ concentrations. Aside from the 1 μM Ag+ linear trendline, which has an R^2 of 0.88, all other fitted trendlines have an R^2 value greater than 0.95.

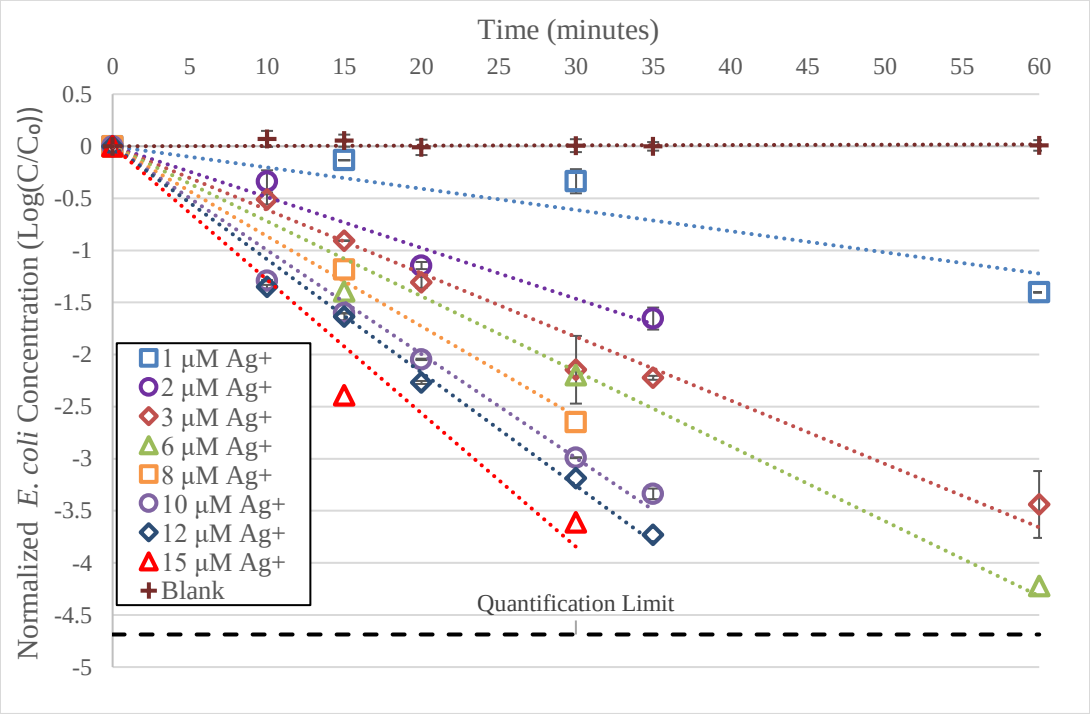

Figure 4.2 *E. coli* 353 TVS inactivation in batch system by several aqueous silver (Ag+) concentrations. Initial *E. coli* concentrations were ~$10^{6.4 \pm 0.3}$ CFU/mL for all experiments. Error bars represent standard deviations.

Given that cell concentrations in Figure 4.2 are log-transformed, the data indicates that *E. coli* 353 TVS inactivation by Ag+ occurs exponentially with *E. coli* concentrations declining rapidly upon first contact with the real-time inactivation rate decreasing exponentially as cell concentrations decline with increased contact time with Ag+. This is consistent with other disinfection studies probing ionic silver's effect on *E. coli* concentrations over time (Hwang et. al, 2007), (Kim et. al, 2008). This is also consistent with Chick's Law which states that "the rate of bacterial

destruction is directly proportional to the number of organisms remaining at any time" (Jorgenson, 1979).

4.1.1 *E. coli* 353 TVS Inactivation Kinetics and Predictive Modeling

With the data obtained from the *E. coli* inactivation experiments using Ag+, it was decided to investigate the inactivation kinetics of Ag+. By converting *E. coli* concentrations to natural logarithmic values and plotting against time for each Ag+ concentration investigated, pseudo first-order inactivation rate constants (min^{-1}) were obtained from the fitted linear trendlines. These pseudo first-order rate constants (blue circles) are shown below in Figure 4.3. Unlike Figure 4.2, where inactivation experiments were averaged for each Ag+ concentration, pseudo first-order rate constants were individually used from each experiment. Therefore, several data points may exist for a single Ag+ concentration.

Upon observing the distribution of the pseudo first-order rate constants, it became clear that a predictive curve could be fit to the data. This would prove useful when analyzing *E. coli* inactivation by Ag/SRB data as the measured Ag+ concentrations could fall within the range of 0-15 μM Ag+. Using Microsoft Excel's SOLVER data analysis add-in package, an optimal curve in the form of a power function with the standard form of $y = a * x^p$ was chosen as the best fit for the data. In this standard form, $\boldsymbol{y}$ is the predicted pseudo first-order rate constant (min^{-1}), $\boldsymbol{x}$ is the Ag+ concentration (μM), and $\boldsymbol{a}$ and $\boldsymbol{p}$ are fitting parameters that remain constant. The fitted power function $y = 0.070 * x^{0.52}$ is plotted below in red in Figure 4.3.

With a high R^2 value of 0.98, this fitted curve can reliably predicted the pseudo first-order inactivation rate constants for micromolar Ag+ concentrations in contact with *E. coli* 353 TVS.

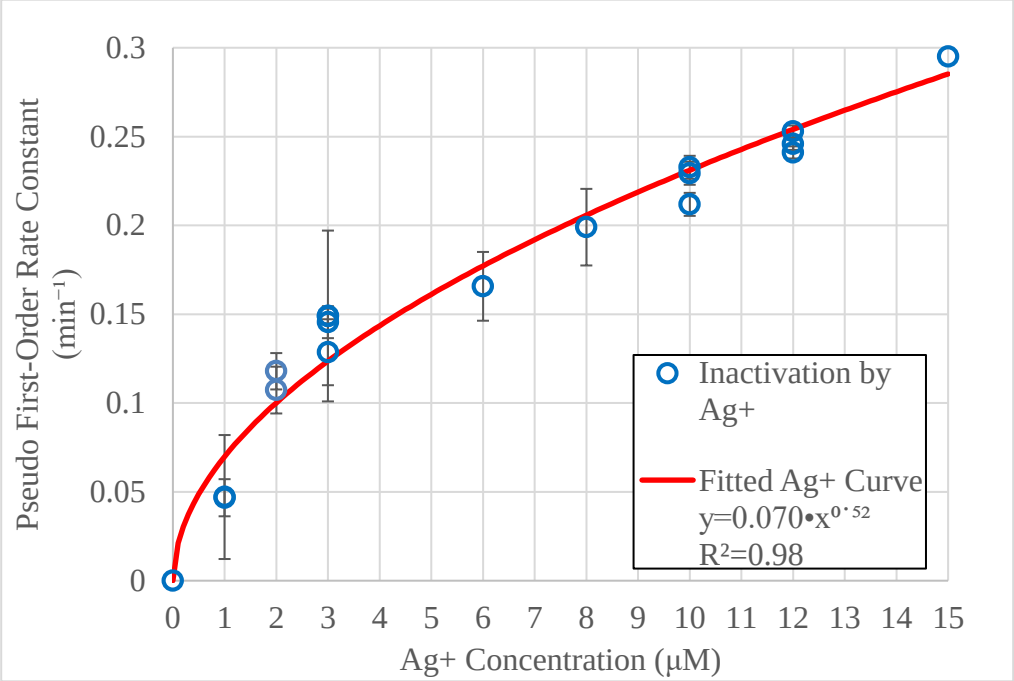

Figure 4.3 Pseudo first-order *E. coli* 353 TVS inactivation rate constants observed from Ag+ inactivation experiments with their corresponding Ag+ concentrations (blue). These rate constants were then fitted to a power function (red) with the form, $y = a * x^p$.

4.2 Batch System *E. coli* 353 TVS Inactivation Experiments using Silver Nanoparticle-Amended Biochar

Silver nanoparticle-amended biochar's biocidal activity was evaluated in batch system to begin determining its potential to serve as an irrigation water treatment media. Several Ag/SRB masses were tested. Unamended air-oxidized SRB served as a control to isolate the effect of the addition of silver to Ag/SRB. A blank containing no biochar of any sort served as the control for the unamended air-oxidized SRB. A ZVI containing reactor was also tested. The results of these batch inactivation experiments are illustrated in Figure 4.4.

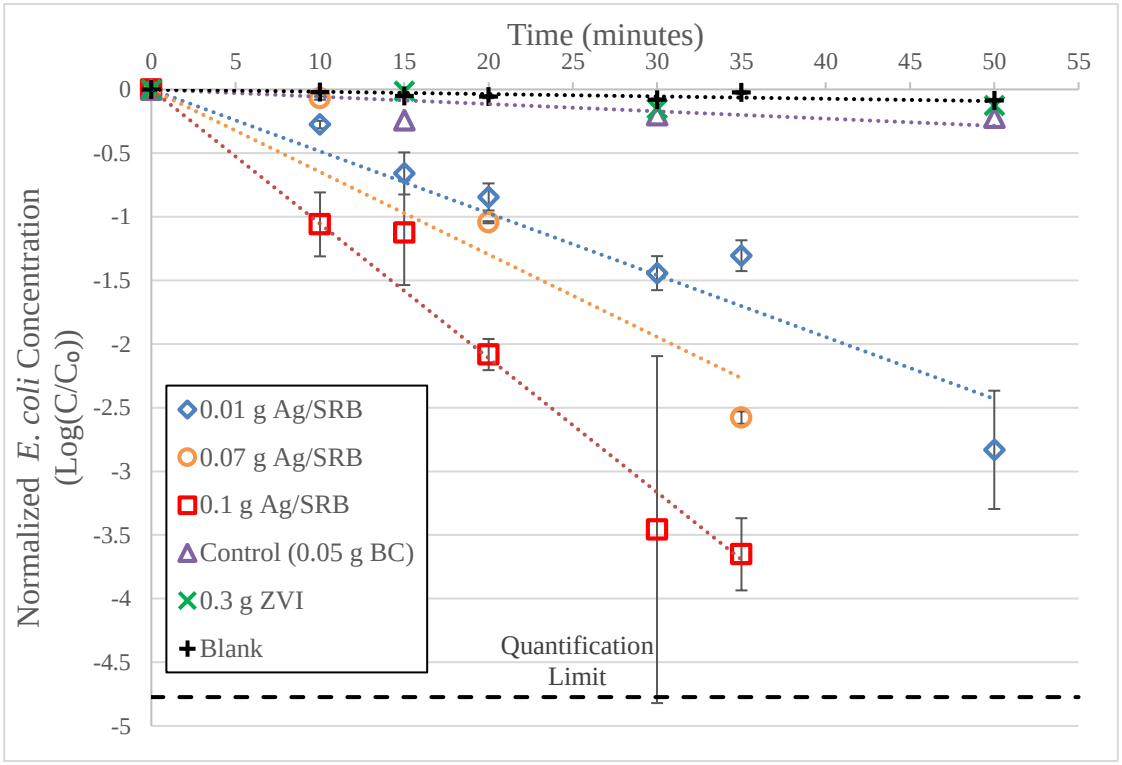

Figure 4.4 *E. coli* 353 TVS inactivation in batch system by several Ag/SRB masses. Initial *E. coli* concentrations were ~$10^{6.4 \pm 0.3}$ CFU/mL for all experiments. Error bars represent standard deviations.

Roughly 1.5 log removal of *E. coli* was observed following 30 minutes of contact time with 0.01 g Ag/SRB, with around 3 log removal seen after exposure to 0.1 g for the same contact time. There was slight removal observed in the control reactor containing unamended SRB as shown in Figure 4.4. This minor concentration decrease is likely due to *E. coli* cells be removed from the general solution due to being sorbed to the biochar surface or due to the *E. coli* cells finding their way into the biochar pores. However, this effect is minimal, thus the removal effect seen with

Ag/SRB exposure can be largely attributed to the silver addition. There was also minimal to no removal observed in the ZVI containing reactor suggesting that ZVI possesses little to no capacity to inactivate *E. coli* cells under batch conditions.

It has been largely agreed upon in the scientific community that the toxicity of silver nanoparticles in aqueous solutions can be attributed to the silver ions produced when silver nanoparticles, which consist of elemental silver (Ag(0)), are oxidized to Ag+ (Zhang et. al 2015). With this in mind, as well as the knowledge gained through the batch Ag+ inactivation experiments, it seemed reasonable that Ag+ concentrations measured in Ag/SRB inactivation and their associated inactivation rates could be compared to inactivation rates determined in the Ag+ inactivation experiments. The results of this comparison are shown in Figure 4.5.

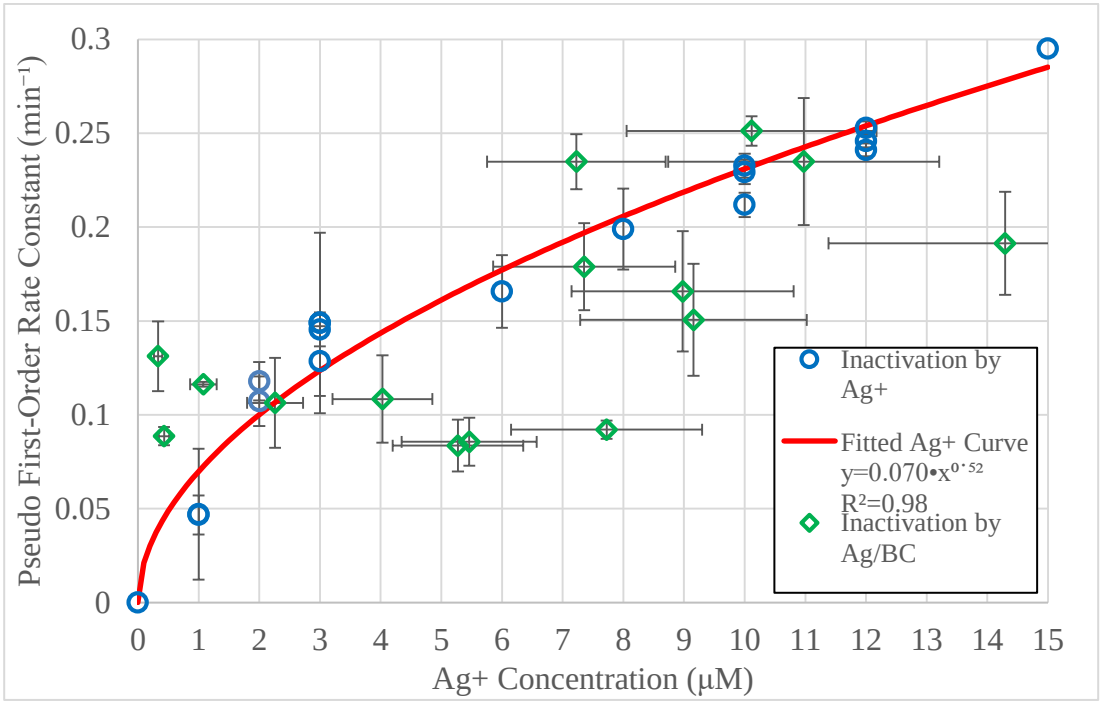

Figure 4.5 Pseudo first-order *E. coli* 353 TVS inactivation rate constants observed from Ag+ inactivation experiments/Ag/SRB inactivation experiments with their corresponding Ag+ concentrations (blue and green, respectively). These Ag+ inactivation experiment rate constants were then fitted to a power function (red) with the form, $y = a * x^p$.

The Ag/SRB inactivation rate constants were paired with the Ag+ concentrations measured halfway through the inactivation experiment. The vertical error bars represent the standard deviations of the measured rate constants, while the horizontal error bars depict the standard deviation of each measured Ag+ concentration due to the use of correction factor to adjust Ag+ concentrations as described in Chapter 3.5.

It can be seen in Figure 4.5, that the Ag/SRB inactivation rate constants are generally grouped around the modelled curve; however, there are several exceptions where the measured Ag+ concentration from a Ag/SRB containing reactor should have produced a higher inactivation rate. These exceptions and the overall lack of a strong correlation with the modelled curve could be due to the heterogeneous nature of Ag/SRB. Silver is not evenly distributed within the biochar pores or on the biochar surface. This heterogeneity could lead to non-constant rates of Ag+ release from Ag/SRB over the course of experiments thus leading to over and underestimation of Ag/SRB performance given a measured Ag+ concentration. However, there is still quite a bit of overlap which supports the conclusion that Ag/SRB toxicity is due to release of silver ion.

4.3 Column Experiments

Given the promising results of the batch Ag/SRB *E. coli* inactivation experiments, the next logical step was to investigate Ag/SRB in a column system. This would provide insight as to how Ag/SRB would function in an actual water treatment system. A sterilized wastewater effluent was used to simulate realistic aqueous conditions under which Ag/SRB could be potentially used to reduce microbial concentrations.

4.3.1 Silver Ion Release from Ag/SRB Under Oxic and Hypoxic Conditions

The EPA has established National Secondary Drinking Water Regulations (NSDWRs). These non-mandatory water quality standards are established as guidelines to assist public water systems in managing aesthetic considerations for their drinking water. Silver is considered a secondary drinking water contaminant, with a secondary maximum contaminant level (SMCL) of 0.1 mg/L (EPA, 2017). While the goal is to assess Ag/SRB's ability to treat irrigation-use water, Ag/SRB may also have the potential to serve as a drinking water treatment media so this comparison may provide ideas as to how to further investigate the potential applications of Ag/SRB.

The goal of this experiment is to determine how or if dissolved oxygen (DO) concentration influences the rate of Ag+ release from Ag/SRB in the short term. To test this, two nearly identical columns were constructed as shown in Figure 3.3 in Chapter 3.7.3. The material components and relevant characteristics of both columns are shown in Table 4.1.

Table 4.1 Column Components and Characteristics (Ag+ Release Experiments)

Component/Characteristic	Column 1 (High DO)	Column 2 (Low DO)
Glass Wool (g)	0.9794	0.9905
Sand (g)	7.6741	7.6785
Ag/SRB (g)	2.0013	2.0096
Pore Volume (mL)	4.975	4.779
Retention Time (min)	1.99	1.91

The experiment was conducted as described in Chapter 3.7.4. The high DO wastewater was pumped through Column 1 with the low DO wastewater being pumped through Column 2. The results of this silver release experiment are shown in Figure 4.6.

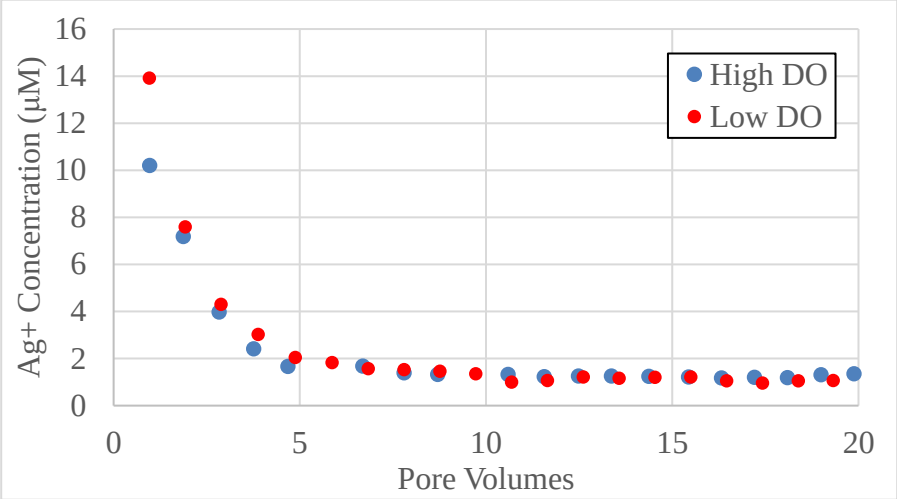

Figure 4.6 Ag+ release from Ag/SRB in a flow-through column system under high and low dissolved oxygen conditions

The results of this experiment show that, in the short term, silver release from Ag/SRB does not depend on dissolved oxygen concentration. This also indicates that very little oxidation of Ag(0) nanoparticles is occurring due to the little difference between the measured Ag+ concentrations following 5 pore volumes passing through each column. This means that the silver being released from Ag/SRB is likely ionic

silver that was sorbed to the biochar surface. The conclusion that DO does not cause significant oxidation of Ag(0) to Ag+ in the short term is further supported when the reaction is analyzed using the Nernst equation. The two reduction half-reactions for this system are shown in Equations 2 and 3 (Stumm and Morgan, 1996).

$$Ag^+ + e^- \rightarrow Ag(s) \text{ (E°= 0.80 V)} \quad (2)$$

$$O_2 + 4H^+ + 4e^- \rightarrow 2H_2O \text{ (E°= 1.229 V)} \quad (3)$$

Solving for the oxidation potentials of the low DO water and high DO water using the Nernst equation, resulted in the potentials, $E_{High\ DO} = -0.6446$ and $E_{Low\ DO} = -0.6235$. Both potentials are similar and both are very close to the reduction potential of Ag(s). This shows that, in the short term, DO concentration does not have a significant effect on the ability for DO to oxidize Ag(s). This also shows that due to the small difference in potential that this oxidation would occur slowly. Other studies support this conclusion, with oxidation of Ag(s) nanoparticles requiring several hours before a significant Ag+ concentration can be measured (Jingyu and Hurt, 2010)

Another interesting observation from this experiment is the stabilizing of the leached Ag+ concentration after roughly 5-7 pore volumes had been pumped through each column. This concentration remains steady for the remainder of the experiment with a Ag+ concentration of ~1.2 μM. This likely occurs because the most easily accessible sorbed Ag+ is easily washed out in the first few pore volumes resulting in the initially high Ag+ concentrations seen in Figure 4.6. Once 5-7 pore volumes have been pumped through, the system appears to approach steady-state, with consistent

flow paths being established resulting in a steady release of Ag+ at a constant rate. This is important as it shows that Ag/SRB can release Ag+ reliably and predictably. It is also notable that this steady-state concentration of 1.2 μM Ag+ converts to 0.13 mg/L, just above the SMCL for Ag+ in drinking water. This indicates that Ag+ removal post-contact with Ag/SRB would be desirable if this technology were to be explored for drinking water treatment purposes. When comparing this steady-state concentration of 1.2 μM Ag+ back to the Ag+ inactivation data in Figure 4.2, it is clear that this Ag+ concentration would be high enough to kill *E. coli* cells. One could also expect that the inactivation would be more pronounced in this column system due to the *E. coli* cells being forced through the Ag/SRB containing layer. The likelihood that an *E. coli* cell would encounter a silver ion would be higher in a column system rather than a batch system. A decreased flow rate and higher silver loading to Ag/SRB would also reasonably increase the leached Ag+ concentration. This could be useful for tailoring Ag/SRB to specific applications and purposes.

As stated, the Ag+ released from Ag/SRB is likely from sorbed Ag+, not silver nanoparticles. When comparing the total silver released in Figure 4.6 to the total Ag+ that can sorb to SRB, 0.267 mmol/g, there is still a large amount of Ag+ sorbed to SRB that could be released through contact with water. For both columns, over 99.5% of the sorbed Ag+ has not been released. This was calculated by fitting a 5^{th} order polynomial to each Ag+ release curve in Figure 4.6 using Excel 2016 and then integrating. This was then compared with the total sorbed silver value for Ag/SRB of 0.267 mmol/g. These results are shown in Table 4.2.

Table 4.2 Calculation of Total Released Silver and Total Sorbed Silver Remaining in Ag/SRB

	High DO	Low DO
Total Ag+ Released (μmol)	1.51	1.92
Total Ag+ Remaining (μmol)	532.84	534.64
Total Ag+ Remaining (%)	99.72	99.64

Assuming that steady release of Ag+ would continue to occur and that all 0.267 mmol/g is accessible, another 380 L (~76,000 pore volumes) of wastewater could be pumped through before fully exhausting the sorbed Ag+ in Ag/SRB. While treating that much wastewater is unlikely, it does indicate that Ag/SRB may be able to function as a long-term filter media. Further long-term trials and field studies would be necessary to fully answer this question.

4.3.2 *E. coli* Removal using SRB and Ag/SRB in a Column System

The final task of this study is to assess the ability of Ag/SRB to remove *E. coli* cells from contaminated water in a column system. Two columns were constructed, one containing Ag/SRB and one containing air-oxidized SRB. The column components and characteristics are shown in Table 4.3. A smaller amount of SRB was used because SRB is less dense than Ag/SRB. This smaller mass, 1.19 g, was calculated by multiplying the Ag/SRB mass, 2.0015 g, by the ratio of the SRB and Ag/SRB densities reported in Table 3.2.

Table 4.3 Column Components and Characteristics (*E. coli* Inactivation Experiments)

Component/Characteristic	Column 1 (Ag/SRB)		Column 2 (SRB)	
	Mass (g)	Volume (mL)	Mass (g)	Volume (mL)
Glass Wool	0.4923	N/A	0.4756	N/A
Sand	7.6640	6.231	7.6868	6.249
Ag/SRB, SRB	2.0015	5.622	1.1907	5.617
Pore Volume (mL)	4.845		5.386	
Retention Time (min)	1.94		2.15	

This experiment was conducted as described in Chapter 3.7.5. The SRB column served as a control. This allows for the difference between the two columns' removal performance to be treated as the direct result of the addition of silver to Ag/SRB. The results of this experiment are shown in Figure 4.7.

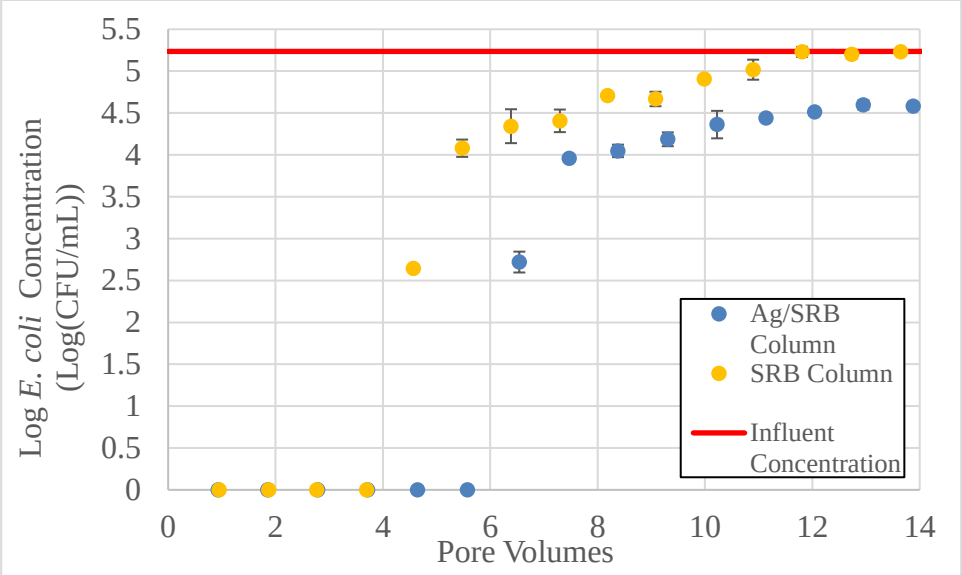

Figure 4.7 Removal of *E. coli* by SRB and Ag/SRB in an upflow column system. $C_o = 1.72 * 10^5$CFU/mL

It can be seen in both columns that *E. coli* cells are retarded given their breakthrough occurs after several pore volumes have passed through each column. Breakthrough occurs in the SRB column after roughly 4 pore volumes have passed through, with breakthrough occurring in the Ag/SRB column occurring after roughly 6 pore volumes. This difference in breakthrough is likely due to the initially high Ag+ concentrations observed when wastewater interacts with Ag/SRB as shown in Figure 4.6 in Chapter 4.3.1. The higher Ag+ concentrations experienced by the first few pore volumes of *E. coli* spiked wastewater could drastically reduce cell concentrations, leading to an apparent delayed breakthrough.

Once breakthrough has occurred, both column effluents begin to show rising *E. coli* concentrations. These concentrations begin to flatten out following passage of roughly 12 pore volumes of wastewater. Following this, the SRB column effluent shows concentrations at nearly the same concentration as the influent concentration. This indicates that, after roughly 12 pore volumes have passed through, full breakthrough has been achieved, with as many *E. coli* cells coming out of the column as there are coming into the column from the influent. This also means that the SRB column components do not have any biocidal effects on *E. coli*. The reductions in *E. coli* concentrations seen in the first 12 effluent pore volumes were then likely due to cell retardation by the column components.

The Ag/SRB column effluent *E. coli* concentrations also levelled off at around 12 pore volumes followed by several data points around a similar cell concentration of roughly 4.5 log. This is in contrast to the SRB column where cell concentrations at these points were around the same as the influent concentration. For this reason, it is reasonable to assume that full breakthrough for the Ag/SRB column occurred following the passage of 12 pore volumes of wastewater. The difference between the two columns' effluent cell concentrations following this, ~0.75 log, can thus be attributed to the silver added to Ag/SRB.

In the *E. coli* batch inactivation experiments using Ag/SRB in Chapter 4.2 and these column inactivation experiments, 100 mL and 70 mL of *E. coli* spiked water was treated, respectively. In batch Ag/SRB inactivation experiments, Ag/SRB was allowed to reach a steady Ag+ concentration before being spiked with *E. coli*. This is similar to

what occurs when the steady 0.75 log removal is observed in Figure 4.7. In both cases, leached Ag+ concentrations have stabilized. Given these similarities it is reasonable to compare Ag/SRB's ability to inactivate *E. coli* in both systems. When comparing the 0.75 log removal which occurred following roughly two minutes of contact time with 2 grams of Ag/SRB in a column system to the results in Figure 4.4, it appears probable that 2 grams of Ag/SRB would be able to remove 0.75 log of *E. coli* cells following 2 minutes of contact time in a batch system as well.

Assuming the ~0.75 log removal is attributed to the steady leached Ag+ concentration seen in Figure 4.6 in Chapter 4.3.1, one could expect this ~0.75 log removal to be observed for many more pore volumes given that a vast majority of the sorbed silver in Ag/SRB would still be available as evidenced from the previous experiment's results in Table 4.2 . This removal efficiency could also likely be improved by either increasing the mass of Ag/SRB in the column or by decreasing the flow rate, thereby increasing the retention time. Further work exploring these different conditions would give a clearer picture of the ability and practicality of Ag/SRB to treat irrigation-use water.

Chapter 5

CONCLUSIONS AND FUTURE RESEARCH

The results of this study show that Ag/SRB does have the potential to serve as an irrigation water treatment media. Ag/SRB's toxicity to *E. coli* stems from release of Ag+ and is comparable to $AgNO_3$-derived Ag+ toxicity. In a batch system with 30 minutes of contact time, 0.1 g/L of Ag/SRB is able to remove 1.5 log of *E. coli* while 1 g/L can remove over 3 log. In a column system, with a short total retention time of roughly 2 minutes, Ag/SRB appears to be able to remove 0.75 log of *E. coli* consistently. These observations show that Ag/SRB does have the potential to be an irrigation water treatment media.

There are still many questions that need answering to better understand Ag/SRB as a water treatment media. Most importantly, longevity is very important for any treatment media. Long-term column experiments should be conducted to measure Ag/SRB's biocidal performance over time as silver nanoparticle oxidation will play a larger role in release of Ag+. To better understand Ag+ leaching behavior, differently silver loaded Ag/SRBs should be tested in flow-through column systems. Different water matrices from contaminated surface waters should be explored as well for treatment to see if there are any differences in Ag/SRB's performance and to better understand the feasibility of using Ag/SRB to treat irrigation water. Ag/SRB's ability to inactivate other microbial pathogens like *Listeria monocytogenes* and *Salmonella* should also be explored. Column experiments should be conducted using different flow rates to determine the impact on Ag+ leaching and removal efficiency. Lastly,

Ag/SRB should be used in a field-scale irrigation water treatment study to assess its performance.

REFERENCES

AGSCO Corporation. (2016, March 4). AGSCO Quartz Technical Data. Retrieved from https://www.agsco.com/assets/pdfs/Quartz-technical-data-sheet-030416.pdf

Bianchini, A., & Wood, C. M. (2003). Mechanism of acute silver toxicity in Daphnia magna. *Environmental Toxicology and Chemistry,22*(6), 1361-1367. doi:10.1002/etc.5620220624

Biswas, P., & Bandyopadhyaya, R. (2016). Water disinfection using silver nanoparticle impregnated activated carbon: Escherichia coli cell-killing in batch and continuous packed column operation over a long duration. *Water Research,100*, 105-115. doi:10.1016/j.watres.2016.04.048

Center for Food Safety and Applied Nutrition. (2018, November 15). FDA Food Safety Modernization Act (FSMA). Retrieved from https://www.fda.gov/food/guidanceregulation/fsma/

CONSERVE. (2016). Retrieved from http://conservewaterforfood.org/

Ding, Z., Hu, X., Wan, Y., Wang, S., & Gao, B. (2016). Removal of lead, copper, cadmium, zinc, and nickel from aqueous solutions by alkali-modified biochar: Batch and column tests. *Journal of Industrial and Engineering Chemistry,33*, 239-245. doi:10.1016/j.jiec.2015.10.007

EPA. (2017, March 08). Secondary Drinking Water Standards: Guidance for Nuisance Chemicals. Retrieved from http://www.epa.gov/dwstandardsregulations/secondary-drinking-water-standards-guidance-nuisance-chemicals

Feng, Q. L., Wu, J., Chen, G. Q., Cui, F. Z., Kim, T. N., & Kim, J. O. (2000). A mechanistic study of the antibacterial effect of silver ions on Escherichia coli and Staphylococcus aureus. *Journal of Biomedical Materials Research,52*(4), 662-668. doi:10.1002/1097-4636(20001215)52:43.0.co;2-3

Fu, F., Dionysiou, D. D., & Liu, H. (2014). The use of zero-valent iron for groundwater remediation and wastewater treatment: A review. *Journal of Hazardous Materials,267*, 194-205. doi:10.1016/j.jhazmat.2013.12.062

Gurtler, J. B., Boateng, A. A., Han, Y., & Douds, D. D. (2014). Inactivation of E. coli O157:H7 in Cultivable Soil by Fast and Slow Pyrolysis-Generated Biochar. *Foodborne Pathogens and Disease,11*(3), 215-223. doi:10.1089/fpd.2013.1631

Hwang, M. G., Katayama, H., & Ohgaki, S. (2007). Inactivation of Legionella pneumophila and Pseudomonas aeruginosa: Evaluation of the bactericidal ability of silver cations. *Water Research,41*(18), 4097-4104. doi:10.1016/j.watres.2007.05.052

Ivask, A., Elbadawy, A., Kaweeteerawat, C., Boren, D., Fischer, H., Ji, Z., . . . Godwin, H. A. (2013). Toxicity Mechanisms in Escherichia coli Vary for Silver Nanoparticles and Differ from Ionic Silver. *ACS Nano,8*(1), 374-386. doi:10.1021/nn4044047

Jorgenson, S. E. (1979). *Studies in Environmental Science*(Vol. 5). Elsevier. doi:doi.org/10.1016/S0166-1116(08)71600-5

Jung, Y., Jang, H., & Matthews, K. R. (2014). Effect of the food production chain from farm practices to vegetable processing on outbreak incidence. *Microbial Biotechnology,7*(6), 517-527. doi:10.1111/1751-7915.12178

Kim, J. Y., Lee, C., Cho, M., & Yoon, J. (2008). Enhanced inactivation of E. coli and MS-2 phage by silver ions combined with UV-A and visible light irradiation. *Water Research,42*(1-2), 356-362. doi:10.1016/j.watres.2007.07.024

Kim, Y., & Carraway, E. R. (2000). Dechlorination of Pentachlorophenol by Zero Valent Iron and Modified Zero Valent Irons. *Environmental Science & Technology,34*(10), 2014-2017. doi:10.1021/es991129f

Komkiene, J., & Baltrenaite, E. (2015). Biochar as adsorbent for removal of heavy metal ions [Cadmium(II), Copper(II), Lead(II), Zinc(II)] from aqueous phase. *International Journal of Environmental Science and Technology,13*(2), 471-482. doi:10.1007/s13762-015-0873-3

Lackovic, J. A., Nikolaidis, N. P., & Dobbs, G. M. (2000). Inorganic Arsenic Removal by Zero-Valent Iron. *Environmental Engineering Science,17*(1), 29-39. doi:10.1089/ees.2000.17.29

Lee, C., Kim, J. Y., Lee, W. I., Nelson, K. L., Yoon, J., & Sedlak, D. L. (2008). Bactericidal Effect of Zero-Valent Iron Nanoparticles on Escherichia coli. *Environmental Science & Technology,42*(13), 4927-4933. doi:10.1021/es800408u

Lehmann, J., & Joseph, S. (2015). *Biochar for environmental management: Science, technology and implementation*. New York: Routledge, Taylor & Francis Group/Earthscan from Routledge.

Leupin, O. X., & Hug, S. J. (2005). Oxidation and removal of arsenic (III) from aerated groundwater by filtration through sand and zero-valent iron. *Water Research,39*(9), 1729-1740. doi:10.1016/j.watres.2005.02.012

Li, C., Wan, Y., Wang, J., Wang, Y., Jiang, X., & Han, L. (1998). Antibacterial pitch-based activated carbon fiber supporting silver. *Carbon,36*(1-2), 61-65. doi:10.1016/s0008-6223(97)00151-6

Liu, J., & Hurt, R. H. (2010). Ion Release Kinetics and Particle Persistence in Aqueous Nano-Silver Colloids. *Environmental Science & Technology,44*(6), 2169-2175. doi:10.1021/es9035557

Liu, Z., & Zhang, F. (2009). Removal of lead from water using biochars prepared from hydrothermal liquefaction of biomass. *Journal of Hazardous Materials,167*(1-3), 933-939. doi:10.1016/j.jhazmat.2009.01.085

Maillard, J., & Hartemann, P. (2012). Silver as an antimicrobial: Facts and gaps in knowledge. *Critical Reviews in Microbiology,39*(4), 373-383. doi:10.3109/1040841x.2012.713323

McDonald, R. I., Green, P., Balk, D., Fekete, B. M., Revenga, C., Todd, M., & Montgomery, M. (2011, April 12). Urban growth, climate change, and freshwater availability. Retrieved from https://www.pnas.org/content/108/15/6312

McDonnell, G., & Russell, A. D. (1999). Antiseptics and Disinfectants: Activity, Action, and Resistance. *Clinical Microbiology Reviews,12*(1), 147-179. doi:10.1128/cmr.12.1.147

Mehra, O. P., & Jackson, M. L. (1958). Iron Oxide Removal from Soils and Clays by a Dithionite-Citrate System Buffered with Sodium Bicarbonate. *Clays and Clay Minerals,7*(1), 317-327. doi:10.1346/ccmn.1958.0070122

Mohanty, S. K., & Boehm, A. B. (2014). Escherichia coli Removal in Biochar-Augmented Biofilter: Effect of Infiltration Rate, Initial Bacterial Concentration, Biochar Particle Size, and Presence of Compost. *Environmental Science & Technology,48*(19), 11535-11542. doi:10.1021/es5033162

Mohanty, S. K., & Boehm, A. B. (2014). Escherichia coli Removal in Biochar-Augmented Biofilter: Effect of Infiltration Rate, Initial Bacterial Concentration, Biochar Particle Size, and Presence of Compost. *Environmental Science & Technology,48*(19), 11535-11542. doi:10.1021/es5033162

Nakhli, S. A., Panta, S., Brown, J. D., Tian, J., & Imhoff, P. T. (2019, March 25). Quantifying biochar content in a field soil with varying organic matter content using a two-temperature loss on ignition method. *Science of The Total Environment,658*, 1106-1116. doi:10.1016/j.scitotenv.2018.12.174

Navarro, E., Piccapietra, F., Wagner, B., Marconi, F., Kaegi, R., Odzak, N., Behra, R. (2008). Toxicity of Silver Nanoparticles to Chlamydomonas reinhardtii. *Environmental Science & Technology,42*(23), 8959-8964. doi:10.1021/es801785m

Nyachuba, D. G. (2010). Foodborne illness: Is it on the rise? *Nutrition Reviews,68*(5), 257-269. doi:10.1111/j.1753-4887.2010.00286.x

Pal, S., Tak, Y. K., & Song, J. M. (2007). Does the Antibacterial Activity of Silver Nanoparticles Depend on the Shape of the Nanoparticle? A Study of the Gram-Negative Bacterium Escherichia coli. *Applied and Environmental Microbiology,73*(6), 1712-1720. doi:10.1128/aem.02218-06

Park, S., & Jang, Y. (2003). Preparation and characterization of activated carbon fibers supported with silver metal for antibacterial behavior. *Journal of Colloid and Interface Science,261*(2), 238-243. doi:10.1016/s0021-9797(03)00083-3

Perlman, H., & USGS. (2016, December 2). Irrigation Techniques. Retrieved from https://water.usgs.gov/edu/irmethods.html

Rangsivek, R., & Jekel, M. (2005). Removal of dissolved metals by zero-valent iron (ZVI): Kinetics, equilibria, processes and implications for stormwater runoff treatment. *Water Research,39*(17), 4153-4163. doi:10.1016/j.watres.2005.07.040

Sharma, M., Millner, P. D., Hashem, F., Camp, M., Whyte, C., Graham, L., & Cotton, C. P. (2016). Survival and Persistence of Nonpathogenic Escherichia coli and Attenuated Escherichia coli O157:H7 in Soils Amended with Animal Manure in a Greenhouse Environment. *Journal of Food Protection,79*(6), 913-921. doi:10.4315/0362-028x.jfp-15-421

Shi, C., Wei, J., Jin, Y., Kniel, K. E., & Chiu, P. C. (2012, January 9). Removal of viruses and bacteriophages from drinking water using zero-valent iron. *Separation and Purification Technology,84*, 72-78. doi:10.1016/j.seppur.2011.06.036

Soil Reef LLC. (n.d.). SOIL REEF™ PURE BIOCHAR. Retrieved from https://www.soilreef.com/product/soil-reef-pure-biochar/

Sondi, I., & Salopek-Sondi, B. (2004). Silver nanoparticles as antimicrobial agent: A case study on E. coli as aBmodel for Gram-negative bacteria. *Journal of Colloid and Interface Science,275*(1), 177-182. doi:10.1016/s0021-9797(04)00163-8

Steele, M., & Odumeru, J. (2004). Irrigation Water as Source of Foodborne Pathogens on Fruit and Vegetables. *Journal of Food Protection,67*(12), 2839-2849. doi:10.4315/0362-028x-67.12.2839

Stumm, W., & Morgan, J. J. (1996). *Aquatic chemistry: Chemical Equilibria and Rates in Natural Waters*. New York, NY: Wiley.

Sun, H., Wang, L., Zhang, R., Sui, J., & Xu, G. (2006). Treatment of groundwater polluted by arsenic compounds by zero valent iron. *Journal of Hazardous Materials,129*(1-3), 297-303. doi:10.1016/j.jhazmat.2005.08.026

Tomás-Callejas, A., López-Velasco, G., Camacho, A. B., Artés, F., Artés-Hernández, F., & Suslow, T. V. (2011). Survival and distribution of Escherichia coli on diverse fresh-cut baby leafy greens under preharvest through postharvest conditions. *International Journal of Food Microbiology,151*(2), 216-222. doi:10.1016/j.ijfoodmicro.2011.08.027

United States Department of Agriculture Economic Research Service. (2019, April 1). Irrigation & Water Use. Retrieved from https://www.ers.usda.gov/topics/farm-practices-management/irrigation-water-use/

Xiu, Z., Zhang, Q., Puppala, H. L., Colvin, V. L., & Alvarez, P. J. (2012). Negligible Particle-Specific Antibacterial Activity of Silver Nanoparticles. *Nano Letters,12*(8), 4271-4275. doi:10.1021/nl301934w

Yao, Y., Gao, B., Inyang, M., Zimmerman, A. R., Cao, X., Pullammanappallil, P., & Yang, L. (2011). Removal of phosphate from aqueous solution by biochar derived from anaerobically digested sugar beet tailings. *Journal of Hazardous Materials,190*(1-3), 501-507. doi:10.1016/j.jhazmat.2011.03.083

You, Y., Han, J., Chiu, P. C., & Jin, Y. (2005). Removal and Inactivation of Waterborne Viruses Using Zerovalent Iron. *Environmental Science & Technology,39*(23), 9263-9269. doi:10.1021/es050829j

Zhang, C., Hu, Z., & Deng, B. (2016). Silver nanoparticles in aquatic environments: Physiochemical behavior and antimicrobial mechanisms. *Water Research,88*, 403-427. doi:10.1016/j.watres.2015.10.025

Zhang, L., & Wang, W. (2018). Dominant Role of Silver Ions in Silver Nanoparticle Toxicity to a Unicellular Alga: Evidence from Luminogen Imaging. *Environmental Science & Technology*,*53*(1), 494-502. doi:10.1021/acs.est.8b04918

Zhou, Y., Gao, B., Zimmerman, A. R., & Cao, X. (2014). Biochar-supported zerovalent iron reclaims silver from aqueous solution to form antimicrobial nanocomposite. *Chemosphere*,*117*, 801-805. doi:10.1016/j.chemosphere.2014.10.057